International Journal of Advanced Pharmaceutical Sciences and Research (IJAPSR)
ISSN: 2582-7618 (Online), Volume-3 Issue-2, February 2023

Review of a Few Selected Examples of Intermolecular Dioxygenases Involving Molecular Oxygen and Non-Heme Iron Proteins

Nasser Thallaj

Abstract: ***Molecular oxygen and non-heme iron proteins (NHIPs) are proteins that have an iron atom bound to one or more oxygen atoms, and are found in bacteria, archaea, and some eukaryotes. NHIPs are involved in a variety of biological processes, such as respiration, electron transfer, and catalysis. They can be categorized into two classes: cytochrome proteins, which are involved in electron transfer, and oxygenases, which catalyze the oxidation of substrates by utilizing molecular oxygen. NHIPs are critical for multiple biological processes, and their impairment has been associated with diseases such as anemia, cancer, and neurological disorders.***

Keywords: Molecular Oxygen And Non-Heme Iron Proteins, Non-Heme Iron-Containing Proteins, Oxygen-Binding Proteins, O_2-Dependent Proteins, Non-Heme Iron Active Sites, Oxygen-Binding Enzymes, Molecular Oxygen Binding Proteins.

I. INTRODUCTION

Molecular oxygen and non-heme iron proteins play a pivotal role in the biochemistry of many organisms, primarily in the generation of energy, the transportation of oxygen and other molecules, and the protection of cells from oxidative damage. The requirement of molecular oxygen for the survival of most living organisms is well-established, and non-heme iron proteins have been extensively investigated for their involvement in processes such as cellular respiration and metabolism. Additionally, non-heme iron proteins have a major part to play in the regulation of gene expression, particularly in plants, wherein the iron-sulfur clusters of the proteins have the capacity to bind to DNA and control its transcription, allowing cells to respond to environmental cues, such as changes in light and temperature, and to other cellular messages, such as hormones. Non-heme iron proteins are also believed to be involved in the regulation of the cell cycle and apoptosis. Despite a great deal of research, the intricate structure of molecular oxygen and non-heme iron proteins is still not fully understood. Investigated structures of certain proteins have revealed the presence of multiple iron types, the most common of which is the heme type, which is usually found in larger molecules and has a strong affinity.

Manuscript received on 02 February 2023 | Revised Manuscript received on 12 February 2023 | Manuscript Accepted on 15 February 2023 | Manuscript published on 28 February 2023.
***Correspondence Author(s)
Prof. Dr. Nasser Thallaj**, Professor, Department of Pharmaceutical Chemistry and Drug Quality Control, Faculty of Pharmacy, Al-Rachid Privet University, Damascus, Syria. E-mail: profthallaj@gmail.com, ORCID ID: https://orcid.org/0000-0002-6279-768X

Among the most studied dioxygenases are certain hydroxylases, such as Phenylalanine Hydroxylase (PAH), Tyrosine Hydroxylase (TyrH) and Tryptophan Hydroxylase (TrpH), as well as α-Ketoglutarate Dioxygenases. This passage provides a thorough overview of the properties of some of the best known examples of these proteins.

1- Overview of Phenylalanine Metabolism

Phenylalanine is an essential amino acid that is essential for human protein synthesis, with a daily minimum requirement of 200-500 mg. Approximately 25% of dietary phenylalanine is incorporated into protein, with the remaining metabolized in the liver. Conversion of phenylalanine to tyrosine is primarily accomplished through the action of phenylalanine hydroxylase (PAH), as shown in **Schema** 1.

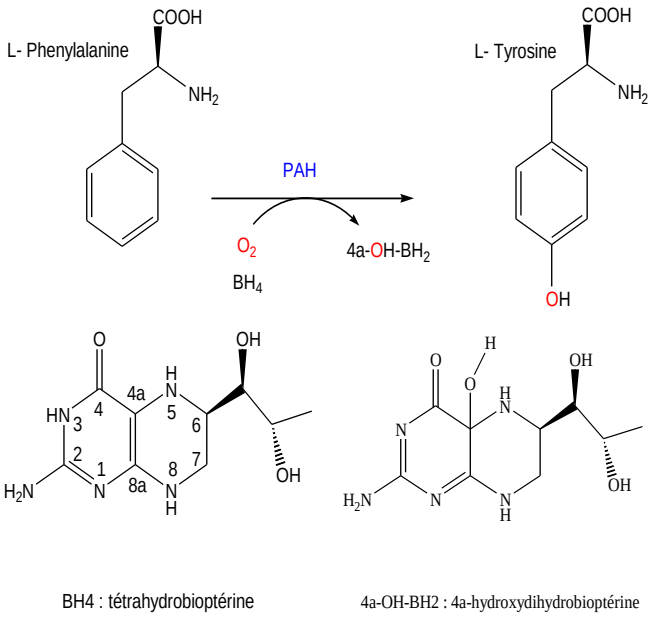

Schema 1: conversion of L-phenylalanine to L-tyrosine by phenylalanine hydroxylase. BH4: tetrahydrobiopterin; 4a-OH-BH2: hydroxydihydrobiopterin.

The enzyme phenylalanine hydroxylase (PAH) consists of a protein component and an essential cofactor, tetrahydrobiopterin (BH4), as an electron source for the hydroxylation reaction. During the reaction, BH4 is oxidized to the quinonoid dihydrobiopterin and a series of reactions ensure its continued recycling [1,2]. Phenylketonuria, a condition caused by PAH deficiency, is characterized by an accumulation of phenylalanine and decreased levels of normal metabolites.

When the level of phenylalanine in the blood reaches 15mg per 100ml, a parallel excretory pathway of phenylalanine in the form of phenylpyruvic acid is generated; this route is minor and only occurs when PAH is functionally impaired.

2- active site of PAH:

Phenylalanine hydroxylase (PAH) was extracted and purified from Escherichia coli. Using X-ray diffraction, the structure of the ferric state of the enzyme was determined, with a resolution of 2 Å, showing that it exists in two dimeric or tetrameric forms, each subunit having a molecular mass of approximately 50 kDa (Figure 1). At the active site, the metal center is situated in an octahedral environment, comprising of two nitrogen atoms from histidines 285 and 290, an oxygen atom from glutarate 330, and three water molecules which complete the coordination sphere, forming a distorted octahedral geometry [3].

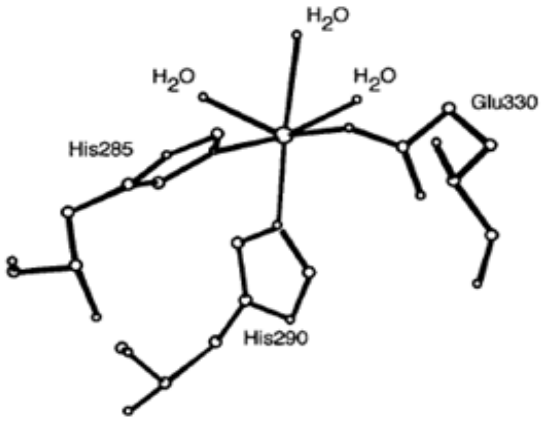

	His_{285}	His_{290}	Glu_{330}	$H_2O(C_{Glu})$	$H_2O(C_{His285})$	$H_2O(T_{His290})$
Fe^{III}	2.2 Å	2.2 Å	2.1 Å	2.3 Å	2.1 Å	2.3 Å

Figure 1: Active site of PAH in ferric state

II. TYROSINE HYDROXYLASE TYRH

1-Overview of Tyrosine Metabolism

Parkinson's disease is a degenerative disorder of the central nervous system that can be treated with medication. This disorder is caused by a decrease in dopamine levels, a hormone derived from the amino acid tyrosine. The production of catecholamines from tyrosine requires the presence of the enzyme Tyrosine Hydroxylase (TyrH) and molecular oxygen, as well as the electron donor coenzyme tetrahydrobiopterin.

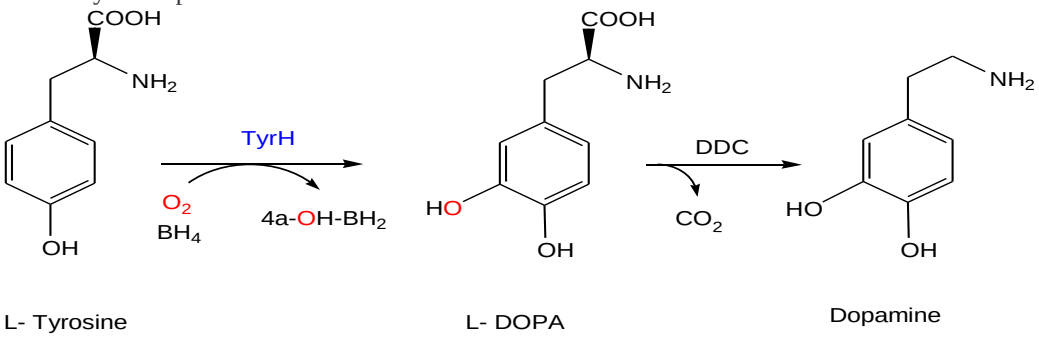

Schema 2: conversion of L-tyrosine to L-Dopa by Tyrosine hydroxylase. BH 4: tetrahydrobiopterin; 4a-OH-BH2: hydroxydihydrobiopterin; DDC: dopa-décarboxylase.

Schema 2 illustrates an aromatic hydroxylation in the α position of a phenol, with the incorporation of an oxygen atom both on the substrate and on the cofactor. This reaction yields L-DOPA, which is then subjected to decarboxylation by the enzyme DOPA decarboxylase, resulting in the production of Dopamine, the precursor of Adrenaline and Noradrenaline.

2-Active site of TyrH

The X-ray diffraction structure of the 7.8 BH2 adducted form of TyrH was determined at a resolution of 2.3 Å, revealing the enzyme to be present in a tetrameric form in solution, with each subunit having a molecular mass of approximately 59 kDa[3,4]. The active site of TyrH was found to be a mononuclear iron center, coordinated by two histidines (His331 and His336), glutamate (Glu376) and two water molecules, Forming a bipyramidal geometry with a trigonal base[3,4]. This finding is consistent with the extraction and isolation of PAH TryH from Escherichia coli.

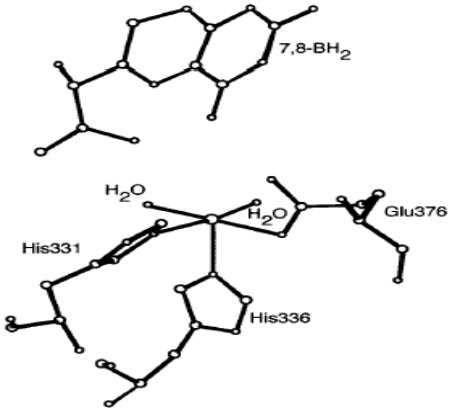

	His_{331}	His_{336}	Glu_{376}	$H_2O(C_{Glu376})$	$H_2O(C_{His331})$
Fe^{III}	2.1 Å	52.1 Å	2.1 Å	2 Å	2 Å

Figure 2: Active site of the adducted form of 7.8 BH2 of TyrH in the ferric state.

Tryptophan Hydroxylase TrpH

1-Overview of Tryptophan Metabolism

The enzyme Tryptophan Hydroxylase (TrpH) catalyzes the transformation of L-Tryptophan into 5-Hydroxytryptophan (5-HT), which is employed in the brain for synthesizing the neurotransmitter serotonin. Serotonin is known to play a role in regulating sleep and is commonly used as an antidepressant.

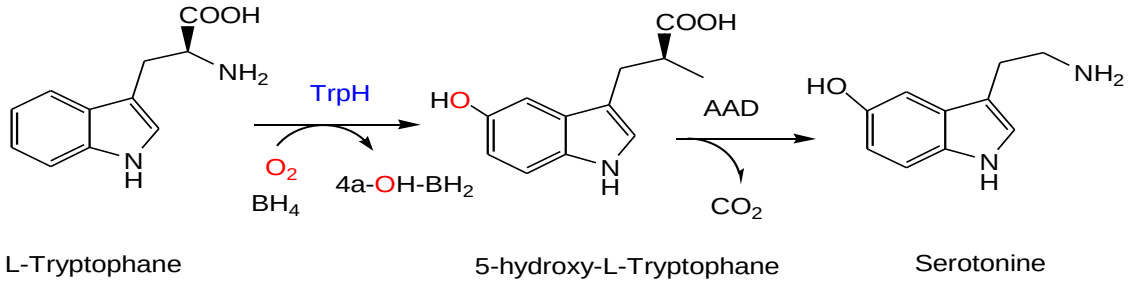

Schema 3: conversion of L-Tryptophan to 5-hydroxy L-Tryptophan by Tryptophan hydroxylase. BH4: tetrahydrobiopterin; 4a-OH-BH2: hydroxydihydrobiopterin;

AAD: Aromatic amino acid decarboxylase.

This process is a hydroxylation reaction, catalyzed by the presence of molecular oxygen, ferrous iron, and BH4 [2].

2- TrpH active site

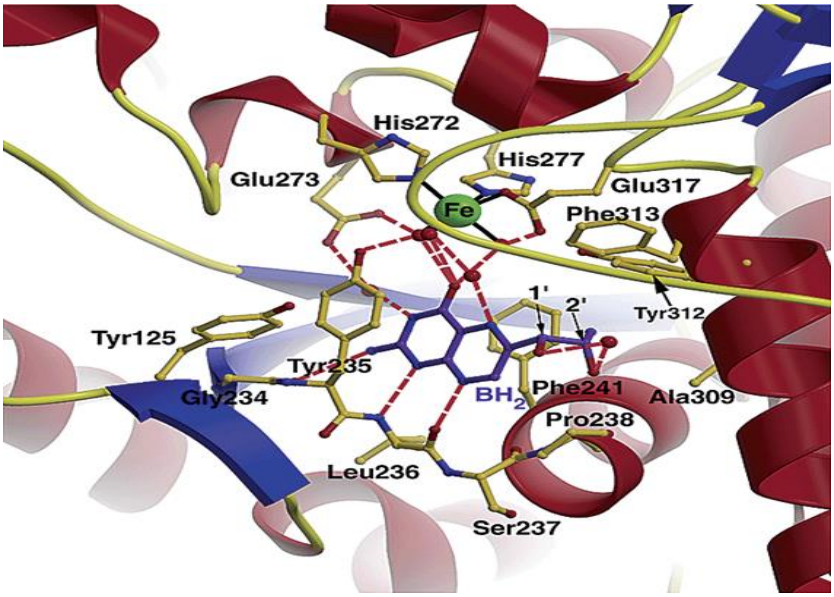

Figure 3: Active site of tryptophan hydroxylase adducted from the 7,8-dihydropterin cofactor according to reference 5.

	His_{272}	His_{277}	Glu_{317}	H_2O_A His272	H_2O_A His277	H_2O_A Glu317
Fe^{III}	2.1 Å	2.0 Å	2.4 Å	2.2 Å	2.3 Å	2.2 Å

The X-ray diffraction structure of TrpH in its ferric state has been determined at a resolution of 1.7 Å. It is an adduct of the oxidized cofactor 7,8-dihydro-L-biopterin, which exists in two dimeric and tetrameric forms. The active site of the adduct consists of two histidines (His272 and His277), a glutamate (Glu317), and three molecules of water, thus forming a deformed octahedron [5].

III. COMMON REACTION MECHANISM OF THESE ENZYMES

It is widely accepted that TyrH, TrpH and PAH possess similar mechanisms of hydroxylation based on sequence and structural homology, and similarity of chemical transformations observed in these enzymes [6]. Mechanistic studies have established that hydroxylation of aromatic molecules requires the presence of both an FeII center and an organic cofactor [1,7]. To date, much of the research on the catalytic mechanisms of these enzymes has been focused on kinetic analyses, including the examination of isotopic effects. Crystallographic studies demonstrated that the active site of both rTyrH and PAH (as well as TrpH) is accessible to the solvent and exogenous ligands, and that a molecule of water can be displaced from the active site upon binding of the pterin ligand. The distance between the iron and the hydroxy carbon of the pterin was found to be greater than 5Å. These findings, combined with previous studies, led researchers to postulate that electron transfer from BH4 to oxygen results in the formation of a superoxide anion as the first reactive intermediate. Subsequently, this radical pair would couple to yield a peroxytetrahydropterin type 4a intermediate. Investigations of rTyrH in the presence of oxygen-18O2[8] appear to indicate the absence of an Fe-oxy intermediate. In this scenario, molecular oxygen is thought to coordinate weakly to a hydrophobic site of the protein situated between the iron and the pterin. The findings of this study, combined with previous research, suggest that the electron transfer from BH4 to oxygen creates a superoxide anion as the initial reactive intermediate. This radical pair would then link to form a peroxytetrahydropterin type 4a intermediate. The structural positioning of pterin in relation to the active site of iron, as observed in the structures of three hydroxylases [5,9,10], suggests that the 4a intermediate peroxytetrahydropterin can coordinate with iron by forming a bridge, as proposed by several groups [1-6]. The iron-peroxypterine that is formed will then be transformed by heterolytic cleavage to yield 4a-HO-BH2 and FeVIoxo, which can then facilitate the hydroxylation of the amino acid.

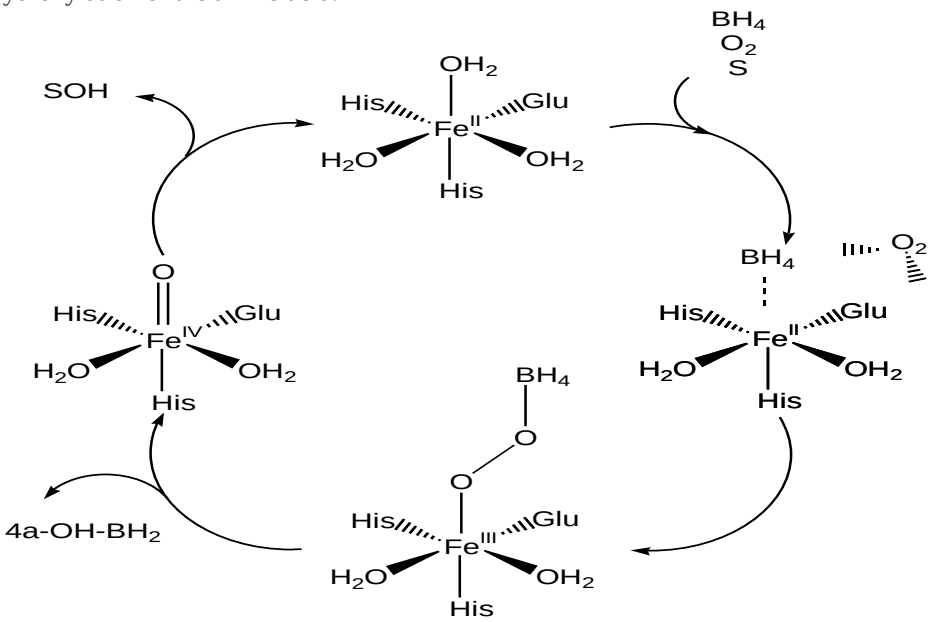

Schema 4: reaction mechanism of the hydroxylation reaction for the three hydroxylases, according to reference 9.

IV. INTRAMOLECULAR DIOXYGENASES

The properties of Lipoxygenase, Intradiol catechol dioxygenase, and Extraradiol catechol dioxygenase, three well-known enzymes in this category, are described below.

Lipoxygenase LOX

1- LOX Metabolism

- Lipoxygenases (LOXs) are non-heme iron dioxygenases which catalyze the regio- and stereospecific hydroperoxidation reaction of 1,4-Z,Z-pentadiene acids[5]. LOXs are ubiquitously distributed amongst plants, animals, algae, mussels, and corals [3]. In mammals, arachidonic acid is the primary substrate of LOXs, while in plants, linoleic acids are typically the predominant substrates.

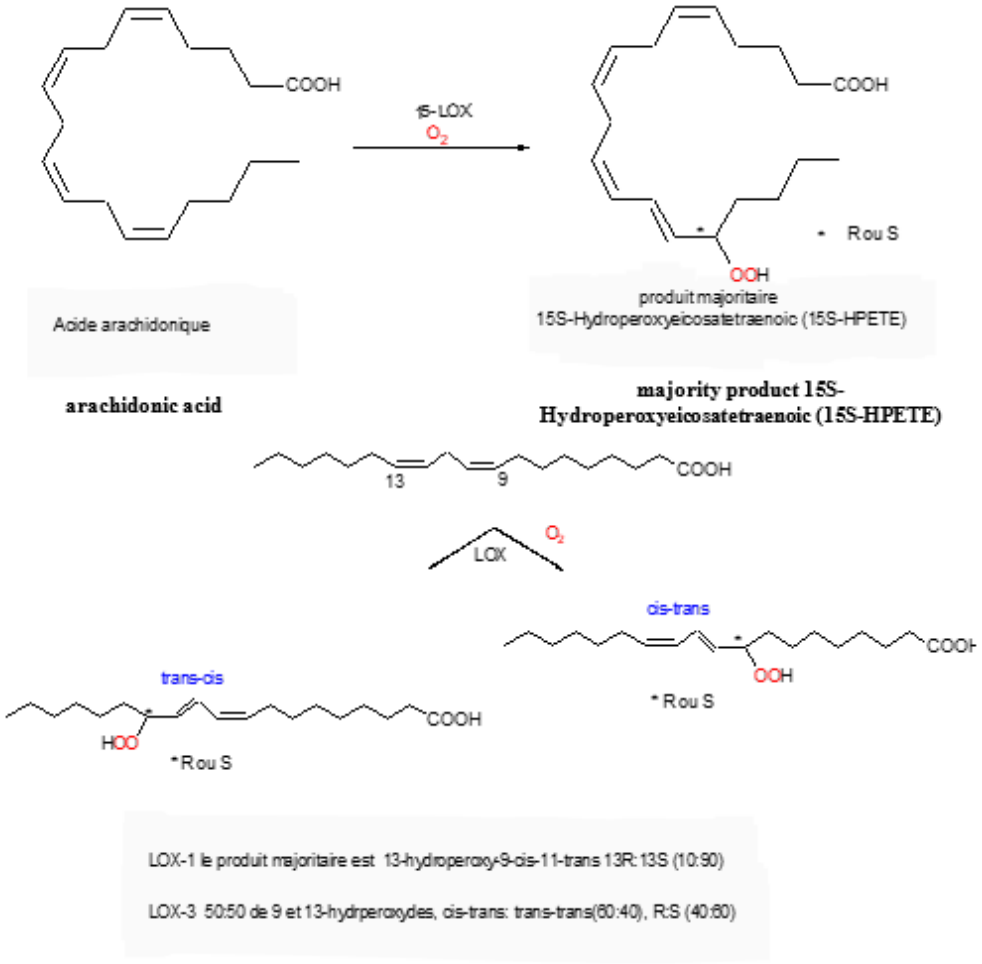

LOX-1 the major product 13-hydroperoxy-9-cis-11-trans 13R:13S (10:90)
LOX-3 50:50 from 9 and 13 hydroperoxy cis-trans:trans-trans (60:40) R:S (40:60)

Schema 5: Reactions catalyzed by the 4 enzymes characterized by X-ray diffraction.

Several types of LOX have been identified, including 5-LOX, which are involved in the biosynthesis of leukotrienes and lipoxins, which are mediators of anaphylactic shock and inflammatory disorders [5-9]; 15-LOX, which are necessary for the initiation of organelle degradation, a pivotal process in certain pathways of differentiation of particular cell types, such as reticulocytes[21]; and 12-LOX, which are implicated in the treatment of cancer cells[2-5]. Three enzymes, SLO-1, SLO-2, and SLO-3, have been isolated from soybeans [2-6]. They demonstrate different pH sensitivities and distinct stereospecific reactivities.

2- Active LOX sites

X-ray diffraction has enabled the obtaining of four distinct structures of SLO-1 at room temperature and a 2.6 Å resolution (SLO-12SBL)[4-7], SLO-1 at 100K and a 1.4 Å resolution (SLO-11YGE)[25], SLO-3 at a 2.1 Å resolution[3] and 15-RLO of rabbit at a 2.4 Å resolution[2-5] (Figure 4). In all of these, the metal is in the ferrous state. The protein environment of soybean lipoxygenases is identical in each of these cases, with three histidines coordinated to the metal and an isoleucine. Moreover, an asparagine is present in each of these examples, however, it is situated in a non-coordinating position with a value close to 3 Å in the best case. The difference between SLO-12SBL and the other two SLOs is that SLO-11YGE and SLO-3 have a weakly bound water molecule in a coordinating position, while 15-RLO has four histidines (361, 366, 541, 545) bound to iron, as well as isoleucine lle663 (linked with the carboxylate oxygen) and a molecule of water or hydroxide in the sixth coordination site [2-14]. The average values of the metal-ligand distances for these SLOs are as follows:

	Fe-N	**Fe-O**		**Fe-N**	**Fe-O**
$SLO\text{-}1_{2SBL}$	2.2 Å	2.1 Å	SLO-3	2.2 Å	2.1 Å
	Fe-N	Fe-O		Fe-N	Fe-O
$SLO\text{-}1_{1YGE}$	2.2 Å	2.4 Å	15-RLO	2.2 Å	2.1 Å

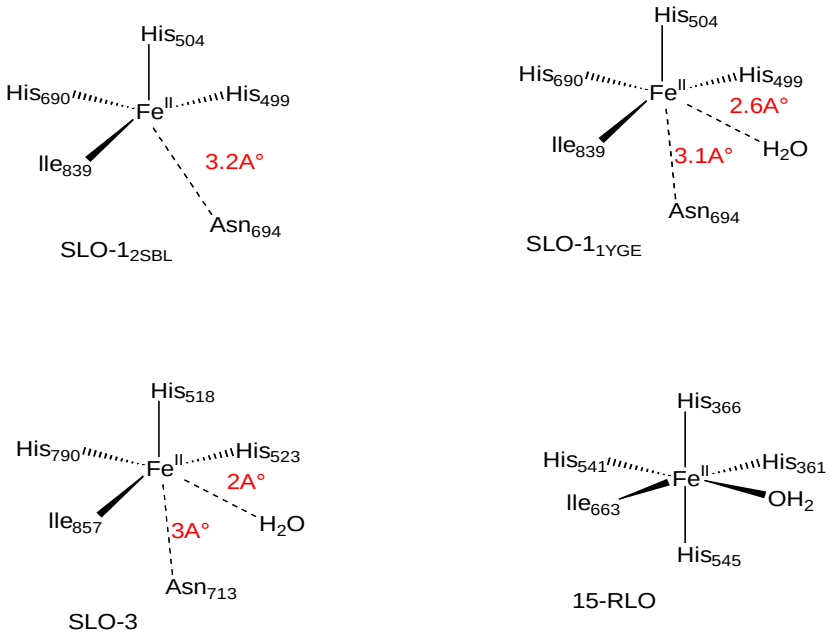

Figure 4: coordination polyhedron at the active site of the lipoxygenases described above.

V. REACTION MECHANISM

The isolated and crystallized species are in a ferrous state, whereas the reactive metallic species are generally in a ferric state. A reaction mechanism has been proposed based on kinetic studies; the pH of these enzymes is typically high, around 9. It is hypothesized that the ferric active site of the resting state is reduced to the ferrous center. Under the reaction conditions, the substrate would experience abstraction of a hydrogen atom, though the intermediate formed has not been identified. The hydrogen atom is then captured by a base in the surrounding medium. It is postulated that the C-H bond undergoes homolytic cleavage, yielding a radical and a metallic species in the ferrous state. [2-6]

The pentadienyl radical generated from the hydrogen abstraction step then reacts directly with dioxygen on the opposite side of the substrate relative to the iron, to form the peroxylyl radical. This radical is postulated to oxidize the ferrous active site to the ferric site, before being reduced to hydroperoxide[2].

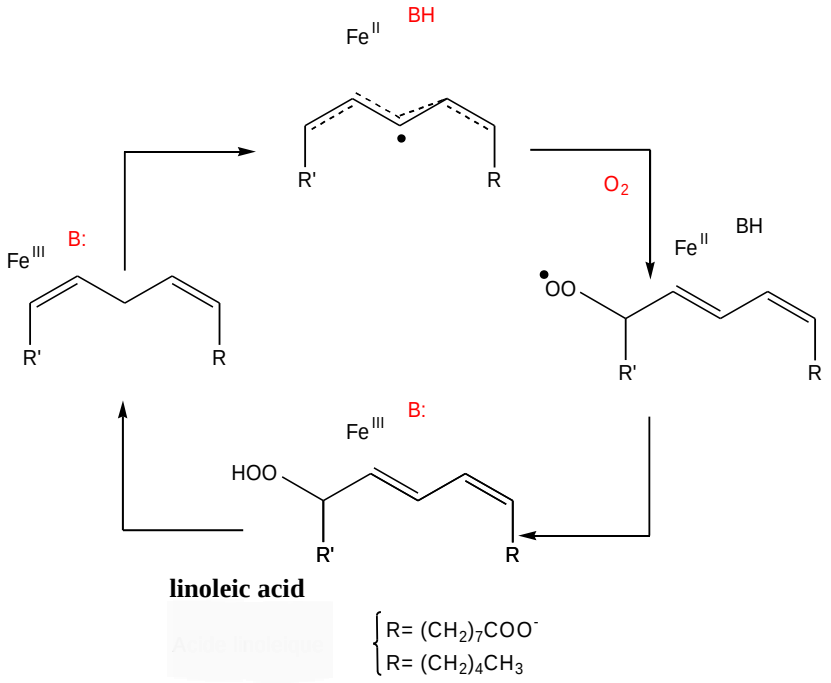

Schema 6: Reaction mechanism of hydroperoxidation of linoleic acid

It should be noted that in this mechanism, the metal acts solely as an activator for the substrate, and there is no evidence of iron coordination to dioxygen.

Catechol Dioxygenase

The degradation of various simple aromatic compounds, such as benzene, toluene, xylene, benzoic acid, phenylacetic acid, and phenylpropionic acid, is carried out by bacteria existing in the soil. It is worth noting that the stabilization energy of a benzene ring in comparison to a cyclic triene is around 150 kJ.mole-1. Therefore, in order to break down the benzene ring, this stabilizing energy has to be overcome in some way. Microorganisms generally use two approaches to accomplish this task.

- Anaerobic bacteria catalyze the reductive hydrogenation of the cyclohexane ring, which is then followed by fragmentation of the backbone.
- Aerobically, the aromatic ring is oxidized to form a dihydroxyaromatic compound (catechol or hydroquinone), and then the ring is cleaved oxidatively. The catechol-type intermediate resulting from this process can be broken down in two ways:

1. intradiol (or ortho cleavage to give muconic acid),
2. or extradiol (or meta cleavage to give hydroxymuconaldehyde acid)

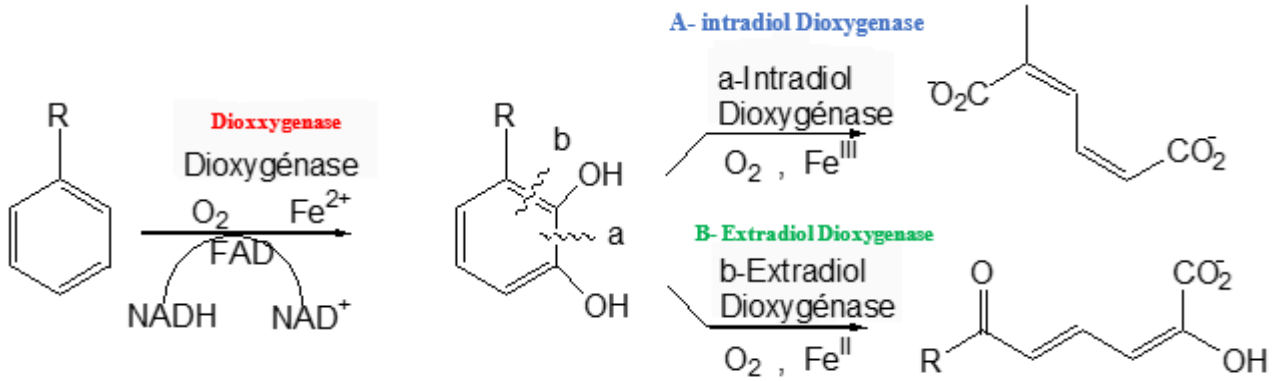

Schema 7 : The catabolic pathways used by bacteria for the degradation of aromatics and catechols.

Oxidative cleavage reactions, such as those presented in Scheme 6, are catalyzed by non-heme iron dioxygenases, termed catechol dioxygenases, discovered by Hayaishi in the 1950s. The non-heme mononuclear iron cofactor can be in the ferric state (intradiol dioxygenases) or the ferrous state (extradiol dioxygenases). [2].

VI. INTRADIOL CATECHOL DIOXYGENASE

1-Metabolism of intradiol catechol dioxygenases

Intradiol dioxygenases catalyze the direct incorporation of the two atoms of dioxygen into the catechol substrate, resulting in an aromatic cleavage between the two hydroxyl groups and the formation of muconic acid. Catechol-1,2-dioxygenase (1,2-CTD) and protocatechuate-3,4-dioxygenase (3,4-PCD) are the best-studied intradiol dioxygenases, with the latter having been intensively characterized by spectroscopy [3]. An X-ray diffraction structure of the coordinated substrateless form of 3,4-PCD from Pseudomonas aeroginosa is now available, providing detailed structural information.

2- 3,4-PCD Active Site

The coordination sphere of the active site of the 3,4-PCD enzyme from Pseudomonas aeroginosa is suggested to have a trigonal bipyramidal geometry, with Tyr447 and His462 occupying the two axial sites, while Tyr408 and His460, as well as an OH ligand derived from water, are located in the equatorial positions[3-7].

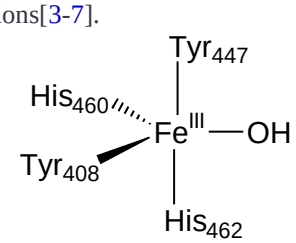

Figure 5: Simplified representation of the geometry at the active site of 3,4-PCD

3- Reaction Mechanism

Spectroscopic studies of the enzyme 3,4-PCD were conducted in the presence of the substrate PCA (protocatechuate). At the outset, the ferric center of the enzyme was reduced by the substrate, which was activated in order to facilitate subsequent electrophilic attack by oxygen. This step was essential, as the ferric state cannot bind molecular oxygen. Spectroscopic and crystallographic studies have demonstrated that the activation of the substrate necessitates the decoordination of Tyr447 and the hydroxyl OH- in the form of H2O[2-8]. Coordination to the metal imparts a radical or anionic character to the substrate, thereby facilitating the direct combination with molecular oxygen [3]. Moreover, the coordination of dioxygen to the metal appears to be essential. A postulated mechanism is illustrated in Schema 8.

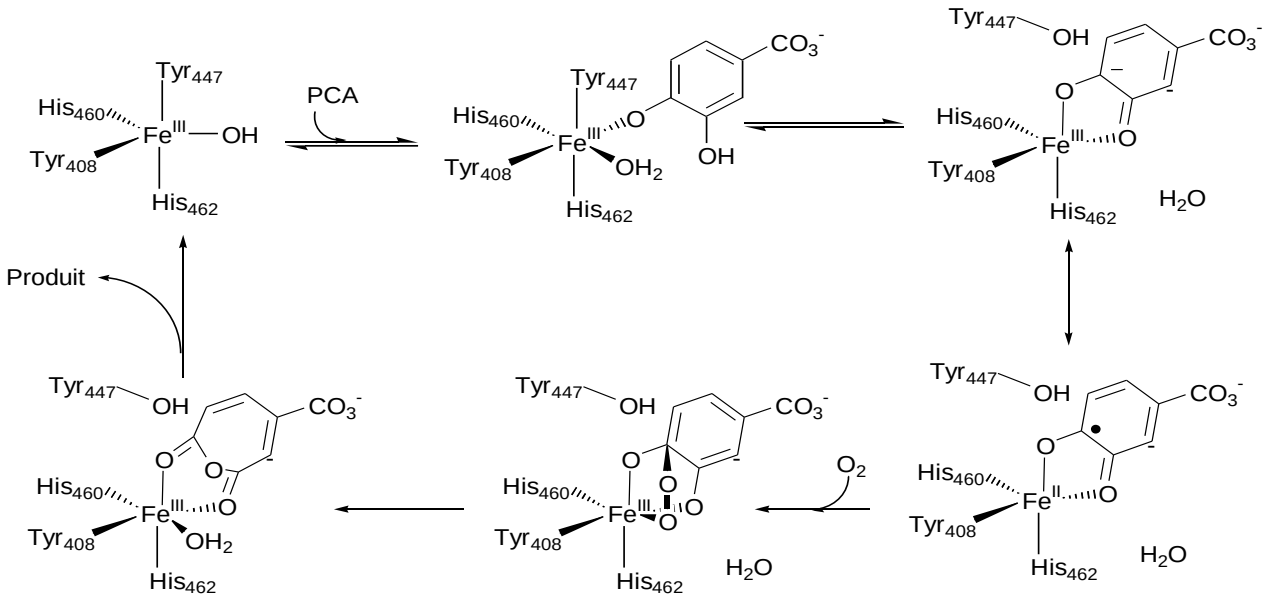

Schema 8: Proposed reaction mechanism for intradiol dioxygenase 3,4-PCD with PCA (3,4-dihydroxyphenylcatechuate).

During the reaction between oxygen and the substrate, a ferric peroxy-type reaction intermediate is formed, which then evolves into a coordinated anhydride. Subsequent hydrolysis of this anhydride yields the desired muconic acid.

Extradiol Catechol Dioxygenase

1-Metabolism of Catechol Dioxygenase Extradiols

The extradiol catechol dioxygenases catalyze the transformation of catechols into hydroxymuconaldehydes via the direct incorporation of two oxygen atoms into the substrate. This is distinct from intradiol catechol dioxygenases, wherein the C-C bond cleavage takes place adjacent to the two hydroxy groups present in the catechol (as depicted in Scheme 7, lane b). A notable example of these enzymes is 2,3-dihydroxybiphenyl 1,2-dioxygenase (BphC), which has been structurally characterized in both the active FeII and inactive FeIII forms by two independent research groups [4-7].

2- BphC active site

Analysis of the two resolved crystallographic structures suggests an active site of square-based pyramidal geometry, comprising of two histidines (146 and 210), glutamate (260) and two water molecules in its coordination sphere.

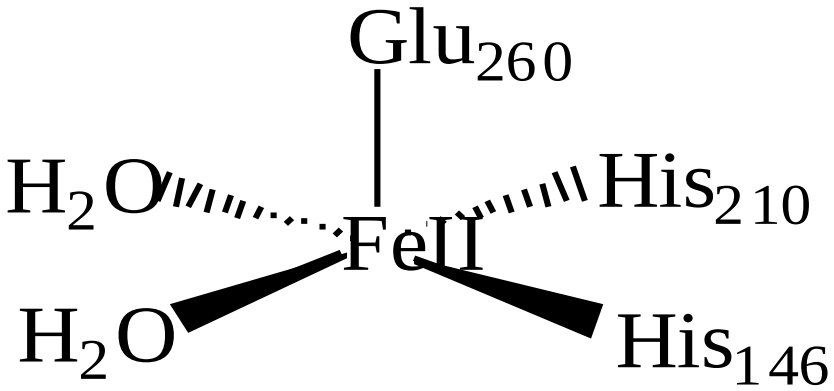

Figure 6: BphC active site

3- Reaction Mechanism

Crystallographic studies have revealed that catechol can adopt a bidentate and anionic coordination [11]. One catechol oxygen atom occupies the vacant sixth coordination site, while the other oxygen shifts the water molecule to the trans position of His210. Additionally, the other water molecule can be lost [12]. According to L.Que, the initial step likely involves the coordination of the substrate to the metal center [9]. Subsequently, the molecular oxygen is coordinated with the iron. The nucleophilic character of oxygen subsequently attacks the carbon atom adjacent to the two hydroxyl groups, leading to the formation of an unstable peroxy intermediate, which undergoes decomposition to generate the product F in schema 9, which then reacts with water to produce the expected product.

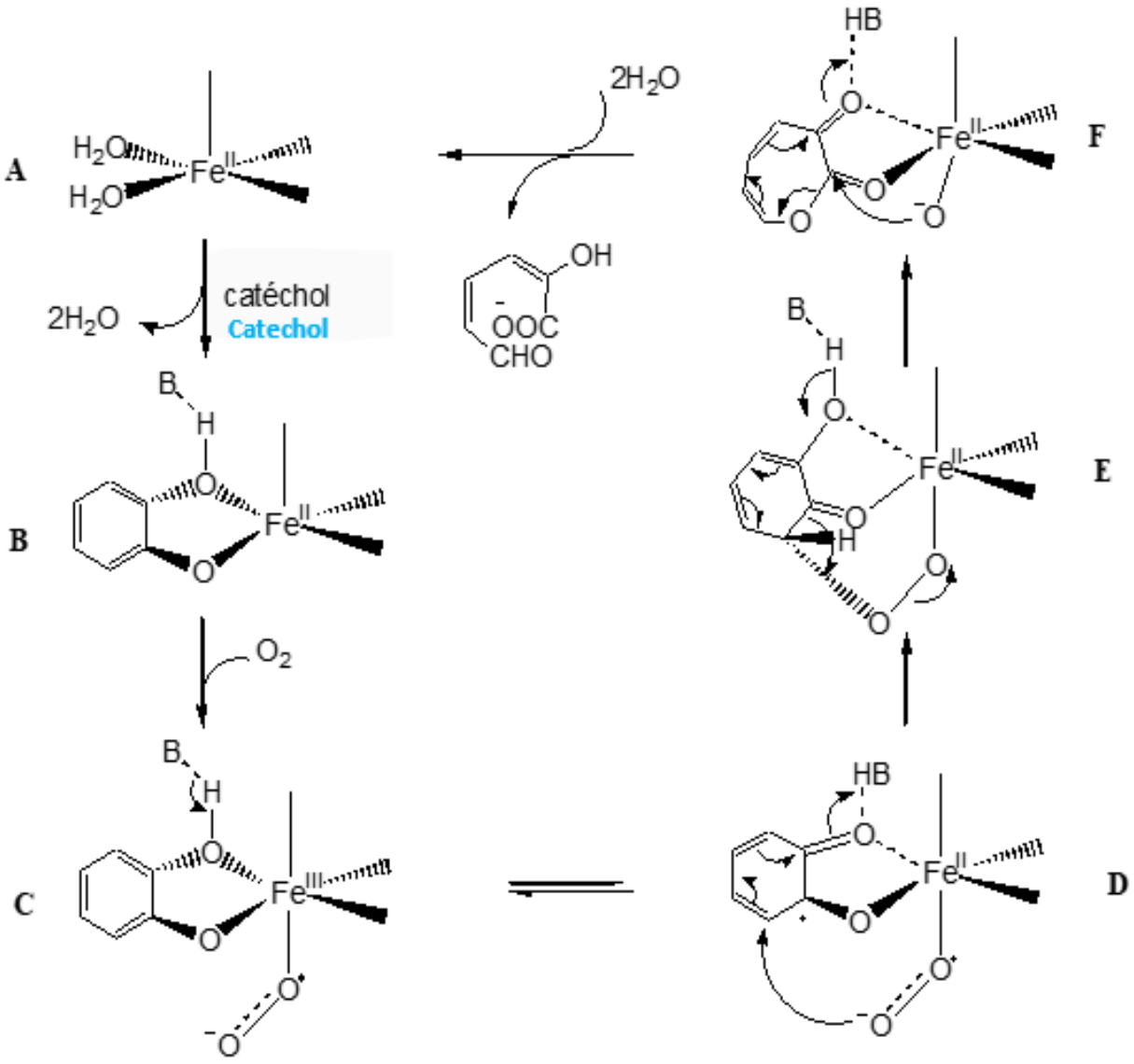

Schema 9 : Reaction mechanism proposed by L. Que for the enzyme BphC with catechol

Oxidases:
Bleomycin

1-Bleomycin Metabolism

Discovered in Japan by UMEZAWA in 1962, Bleomycin A2 is the most extensively studied form of the glycopeptide antibiotic produced by fermentation of Streptomyces Verticullius. It is commonly used to treat various types of cancer, including Hodgkin's disease, lymphomas, head or testicular cancers[7-10].
Therapeutic activity is thought to be associated with the capacity to bind and degrade DNA. Several studies have demonstrated that the degradation of DNA necessitates the joint presence of molecular oxygen and a FeII metal ion [13-16].

2- Active site of bleomycin

The crystal structure of the ferric complex has yet to be determined by radiocrystallography, while that of the cupric (CuII) complex has been established. Furthermore, model complexes of cobalt (CoIII) and zinc (ZnII) have been investigated through spectroscopic and theoretical approaches, both in the absence and presence of molecular oxygen [12-16].
Bleomycin is made up of three parts:
• A complexing active site containing three amides and two amines from the β-hydroxyhistidine, pyrimidinyl proionamide, and β aminoalanine groups;
• a peptide region extended by a bithiazole;
• a sugar region extended by a potential ligand of the carbamoyl type [6-10].

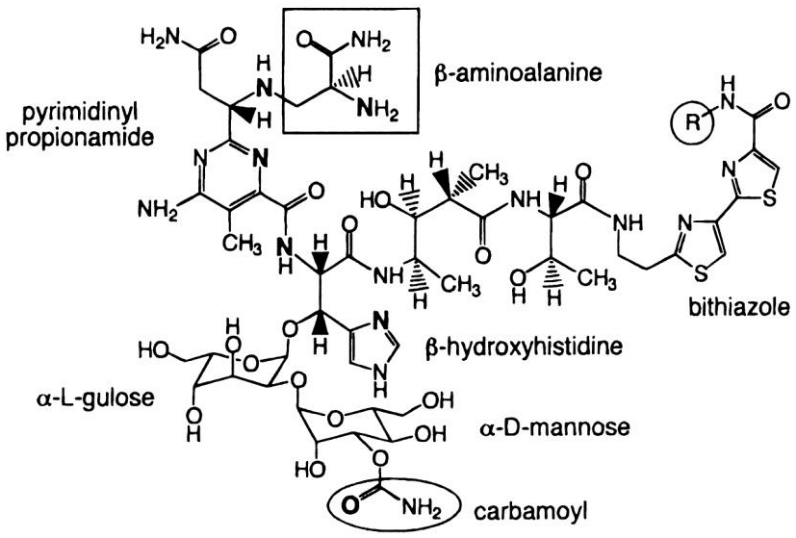

Schema 10: Bleomycin molecule

3- Reaction Mechanism

Two hydrogen bonds between the pyrimidine moieties of bleomycin and the guanine residues of DNA have been shown to be necessary for bleomycin reactivity [18-22]. The initial reaction of ferrous bleomycin (FeIIBLM) with molecular oxygen (O2) results in the formation of an oxygenated bleomycin species (BLMFeIII-O2-). This is followed by either a further reduction from an additional oxygenated bleomycin molecule, leading to the formation of FeIIIBLM + O2, or from other reducing agents present in the medium, such as superoxide or peroxide species. This is then followed by the generation of BLMFeIII-OOH, at which point the DNA degradation process begins. The ongoing debate surrounding the active species of the reaction involves the hydroperoxide BLMFeIII-OOH, which could be the cause of the abstraction of hydrogen C4-H from deoxyribose from DNA [7]. Additionally, experiments utilizing oxygen-18O2 have suggested that degradation could occur through the heterolytic cleavage of the O-O bond [8].

This suggests that there are two potential pathways: a direct reaction between the BLMFeIII-OOH species and deoxyribose, resulting in the formation of a deoxyribose radical, and another pathway in which a highly oxidizing BLMFeIVoxo species is responsible for the breakdown of DNA.

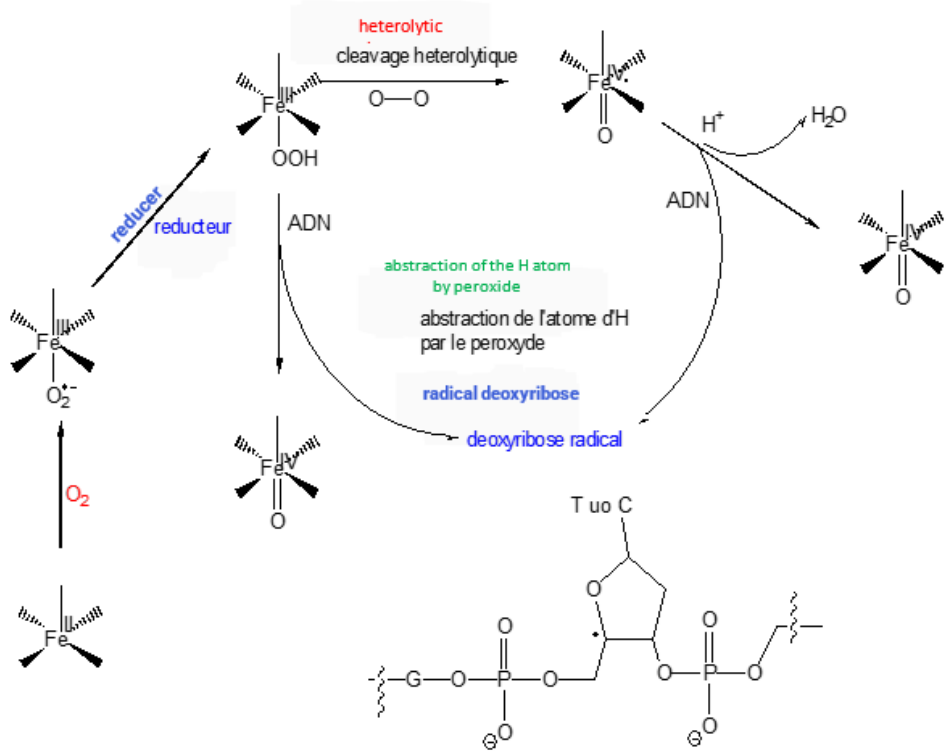

Schema 11: Bleomycin Reaction Mechanism

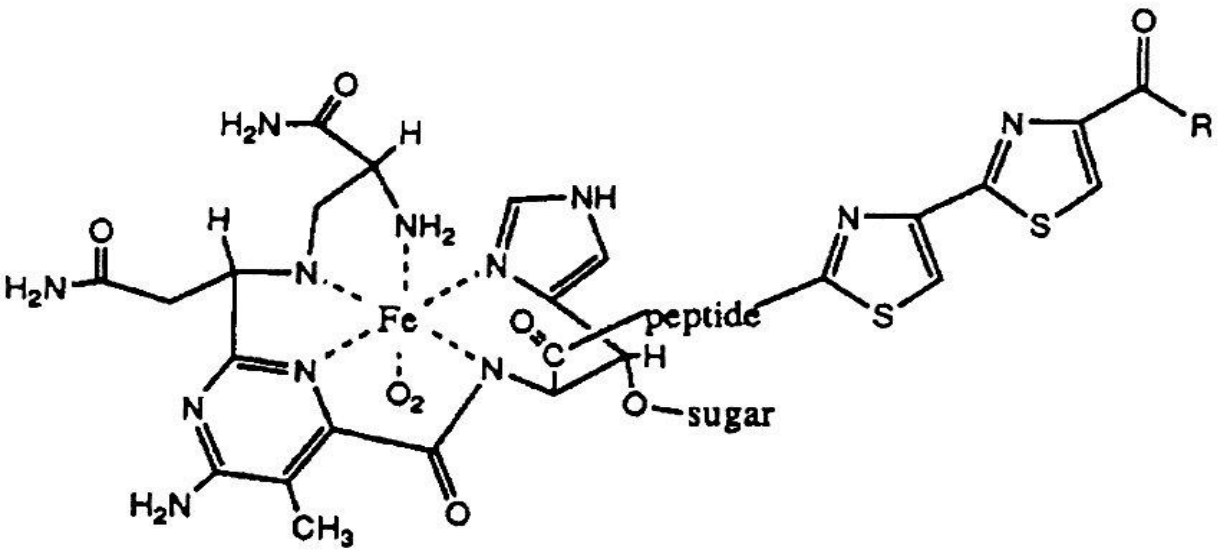

Figure 6: active site of Fe^{II}BLM in the presence of molecular oxygen according to Stubbe.

Isopenicillin N synthase IPNS

1-IPNS metabolism

Research into the chemistry of penicillins and cephalosporins is essential in order to gain insight into their formation mechanisms. It is known that the biosynthesis of these antibiotics in certain microorganisms involves oxidative reactions which convert δ-(L-α-aminoadipoyl)-L-cysteinyl-D-valine (ACV) into isopenicillin N, the precursor to penicillins and cephalosporins. This results in the formation of two β-lactam and thiazolidine rings.

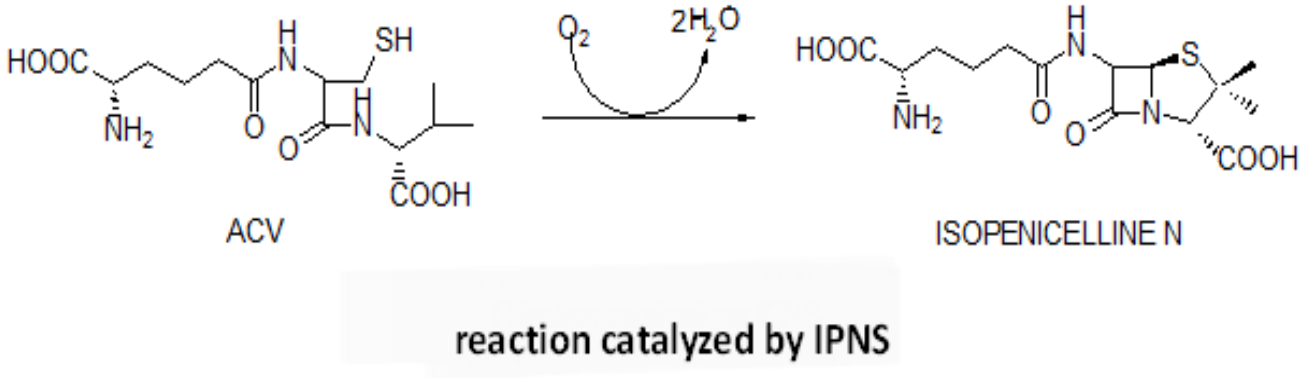

Schema 12: Biosynthesis of isopenicillin N

The conversion of ACV peptide into isopenicillin is catalyzed by isopenicillin N synthase (IPNS), which requires the presence of FeII and molecular oxygen (O2) for its activity. This process is an example of an oxidase reaction[10-22].

2-IPNS active site

The X-ray crystal structure for the FeII-MnII complex, determined by Roach et al. in 1995 [4-10], exhibited a coordination sphere comprising of four protein residues (two histidines, an aspartate, and a glutamine) and two water molecules. This structure corroborated the biological and spectroscopic research findings on the ligands around the metal site. Under anaerobic conditions, X-ray crystallographic analysis of the ACV enzyme-peptide adduct revealed the departure of an amino acid Gln330 and a molecule of water. This structure noted a transition from an octahedral geometry to a pentacoordinated geometry, with the coordination sphere consisting of two histidines, an aspartate, a water molecule, and ACV connected through the sulfur atom[12]. The coordination of acetyl-CoA thiolate to Fe(III) pyridinethiosemicarbazone (IPNS) had been previously suggested by a number of spectroscopic studies [17-18]. The enzyme became oxygen-sensitive only after the acetyl-CoA peptide (ACV) coordination, however, the adduct proved to be unstable. Consequently, studies were conducted on the enzyme in the presence of nitric oxide (employed here as an oxygen analog) and the ACV peptide [22]. Single crystals were obtained and the X-ray crystal structure of the Fe(II).ACV.NO.IPNS complex displayed the presence of NO in the trans position of Aspartic Acid (Asp) 216. This hints to the coordination of the oxygen molecule in the trans position of Asp 216 to promote the formation of the thiazolidine ring.

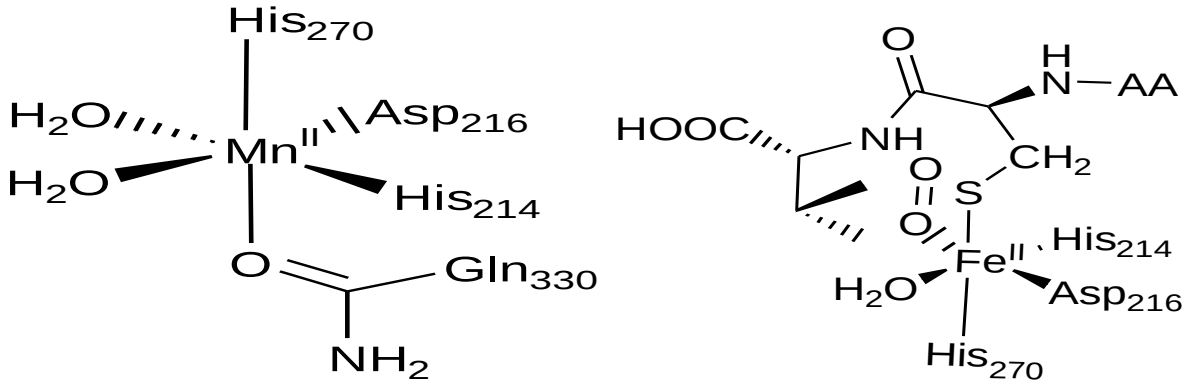

Figure 7: (A) active site of IPNS. MnII; (B) The coordination sphere of the Fe^{II} center in the presence of ACV and O_2.

3- Reaction Mechanism

Based on reactivity studies conducted by Baldwin, it has been proposed that acetoxycyclohexanecarboxylic acid (ACV) and oxygen are coordinated consecutively at the center of FeII [6]. Moreover, the key steps in obtaining the product involve the formation of two β-lactam and thiazolidine rings via oxidative processes. To further corroborate these findings, two experiments were conducted using modified peptides in lieu of ACV. The compound AcmC, in which the D-Valine of ACV was replaced by D-S-methyl-cysteine, was employed in order to bolster the hypothesis of the presence of an FeIV-oxo intermediate. This was done by attempting to inactivate its physiological activity through the formation of a sulfoxide. This approach was successful and was observed in [7-13].

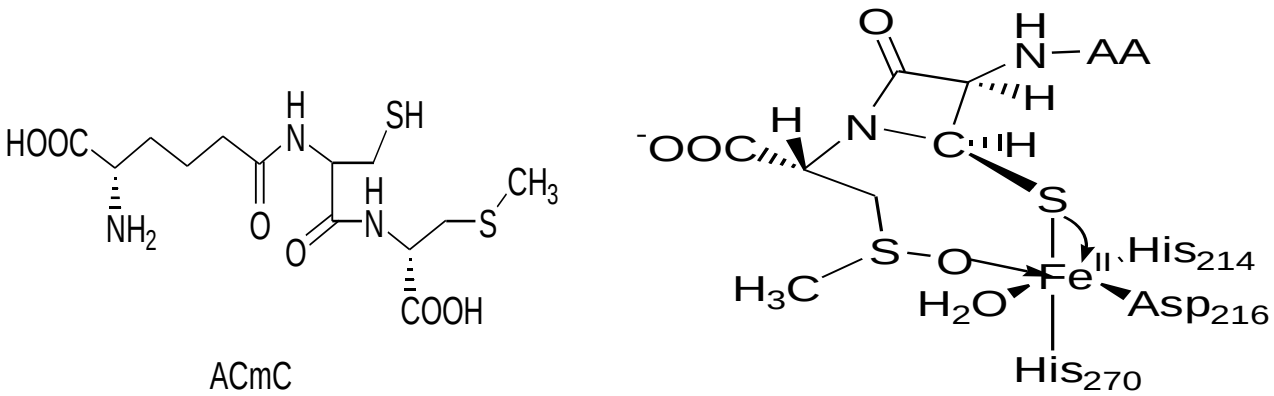

Schema 13: The ACmC peptide and its reaction product with IPNS: absence of cyclization

In order to gain insight into the formation of the β-lactam ring, a fluorinated peptide, which is resistant to oxidation, was used in the experiment. Under the enzyme's operating conditions, cyclization was not observed and the resulting product was a thioacid [10].

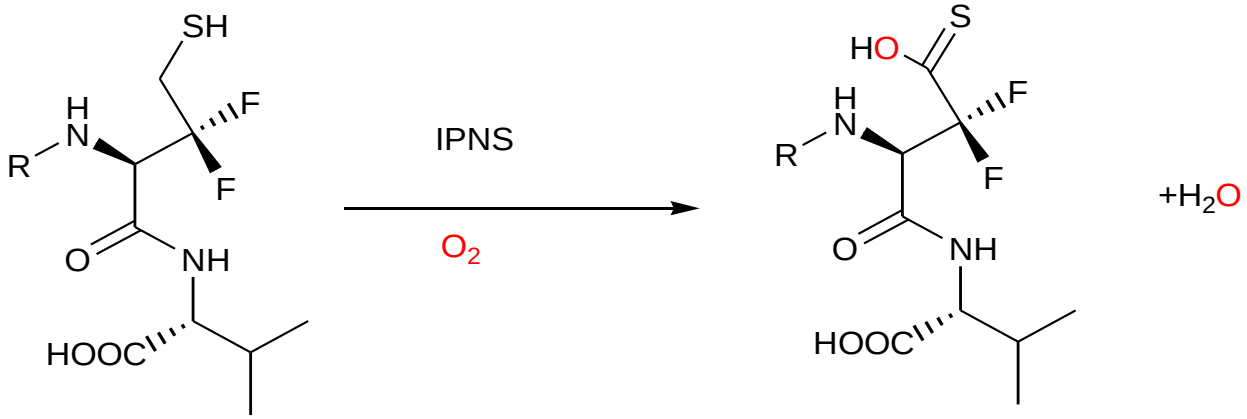

Schema 14: the ACV analogue with a difluoro-cysteine fragment and the thioacid obtained by its reaction with IPNS in the presence of molecular oxygen.

The proposed reaction mechanism involves the coordination of molecular oxygen to ferrous iron, followed by the involvement of an oxo species with a high oxidation state of iron (Fe(IV)) [10-13].

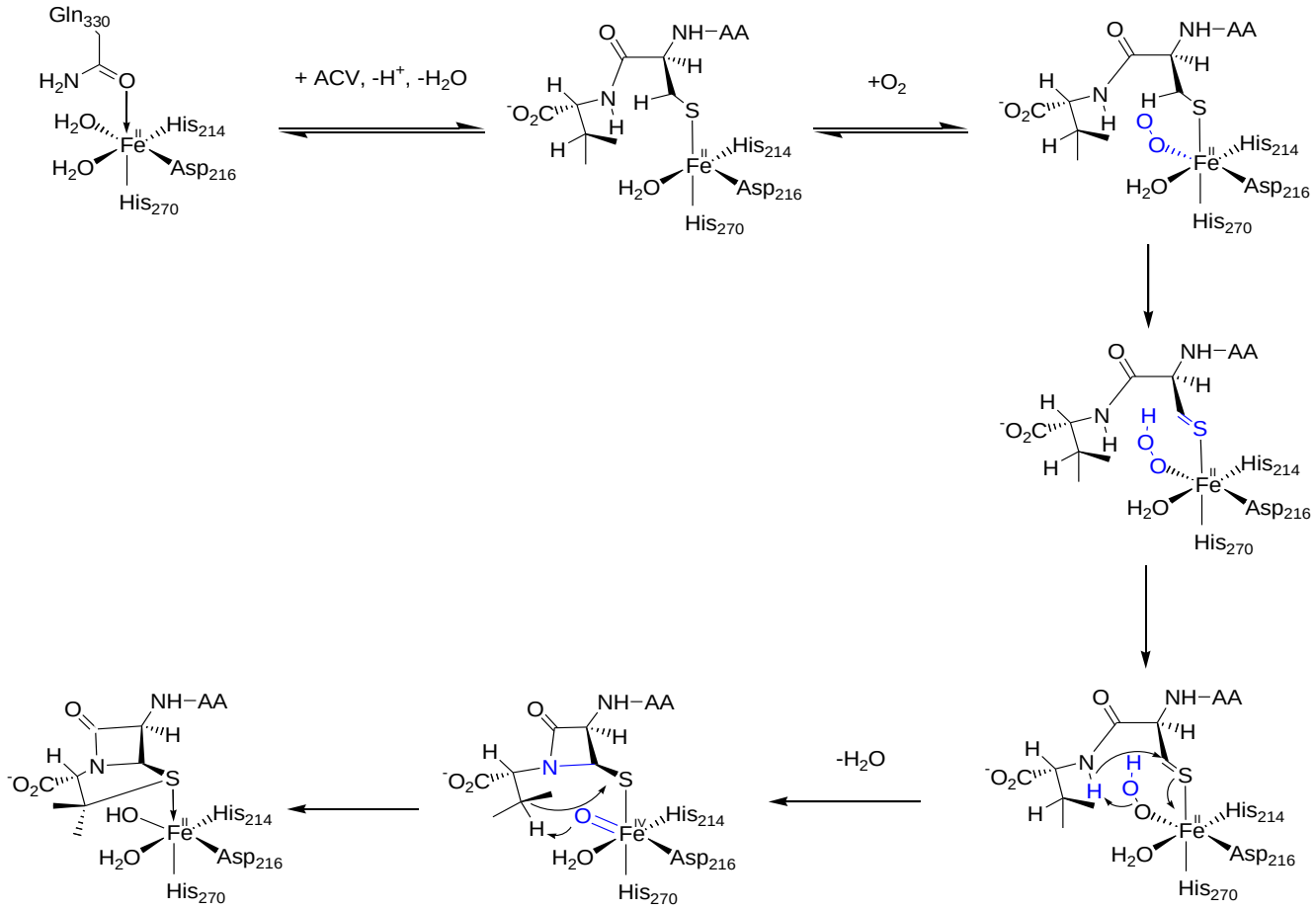

Schema 15: Reaction mechanism of IPN biosynthesis

Monooxygenases

Methane Monooxygenase, MMO

1- Ecology

Methane, a biologically-derived gas, is produced by methanogenic bacteria in anaerobic environments. After carbon dioxide (CO2) and freons, it is considered to be the third most significant contributor to global warming due to its ability to absorb infrared radiation, which gives it a greater warming power than CO2. Additionally, its presence in the atmosphere reduces the capability of oxidizing tropospheric pollutants such as freons, thus contributing to the depletion of the ozone layer, which is a critical component of life on Earth as it absorbs ultraviolet radiation.

The presence of both oxygen and methane simultaneously, generated by anaerobic organisms, fosters the growth of aerobic bacteria - known as methanotrophs - which metabolize methane and convert it into methanol by cleaving the C-H bond of the methane molecule. This bond is particularly difficult to break down due to the substantial dissociation energy of approximately 104 kilocalories per mole.

$$CH_4 + NADH + H^+ + O_2 \longrightarrow CH_3OH + NAD^+ + H_2O$$

The degradation of methanol involves its conversion to formaldehyde via dehydrogenation, catalyzed by a dehydrogenase. This reaction uses NAD+ as a cofactor, and produces formate as the product, which is then converted to carbon dioxide (CO2). This process allows methanotrophs to use methane as their sole source of carbon and energy for growth and survival [12-19].

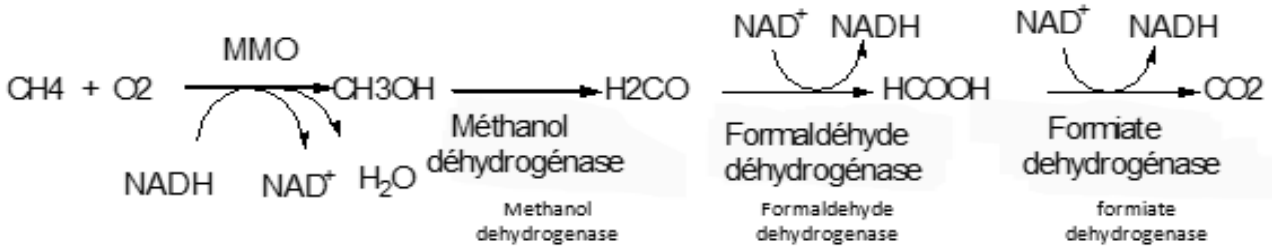

Schema16 : Methane oxidation metabolism by methanotrophic bacteria.

Methanotrophic bacteria utilize an enzyme known as methane monooxygenase (MMO) for the hydroxylation of methane. Two distinct forms of MMO have been identified; the first form is an enzyme that is found in habitats with a high concentration of copper [17-22]. The active site of the enzyme consists of three atoms of a certain metal; however, further discussion of this is beyond the scope of this text. The second form of the enzyme, referred to as soluble methane monooxygenase (sMMO), is found in media with a high concentration of iron. Almost all methanotrophs express the copper-containing pMMO enzyme. In certain methanotrophic organisms, the expression of the soluble sMMO form has also been observed, such as in Trichosporon methylosinus and Methylococcus capsulatus [22-29]. Unlike pMMO, sMMO is much more stable and easier to purify from a structural standpoint [28-32].

2-Structure Tridimentionnelle

Methane monooxygenase (MMO) is a tripartite enzyme composed of three proteins: MMOR (38.5 kDa), MMOB (15.5 kDa), and MMOH (251 kDa). MMOR is a reductase, MMOB is a coupling protein, and MMOH is a hydroxylase.

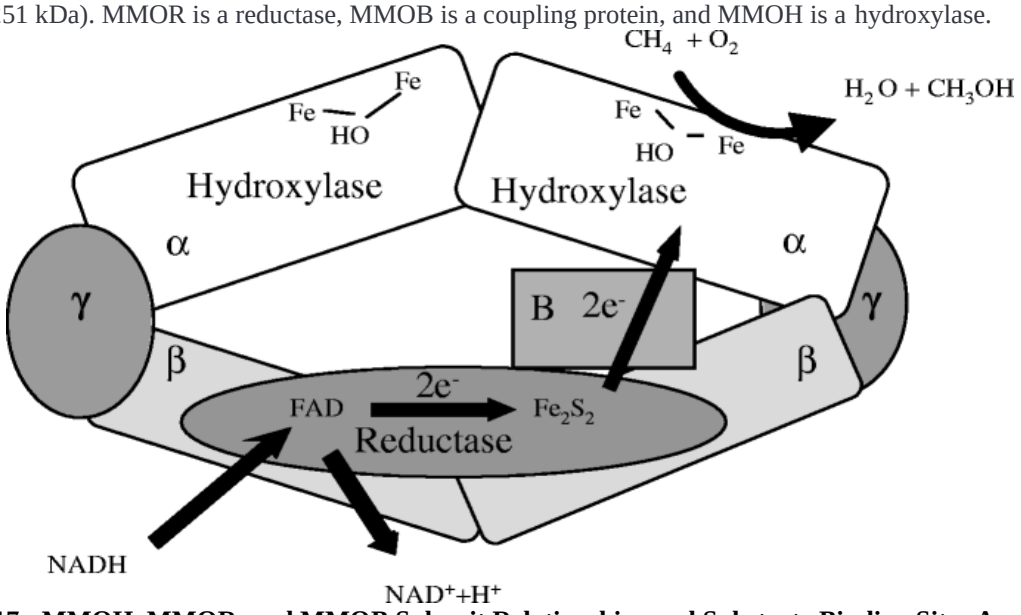

Schema 17 : MMOH, MMOR, and MMOB Subunit Relationships and Substrate Binding Sites According to Reference 32

MMOR (Membrane-Bound Oxidoreductase) facilitates the transfer of two electrons from NADH (Nicotinamide Adenine Dinucleotide) to MMOH (Methyl Viologen) through the use of two prosthetic groups: an Fe2S2 cluster and FAD (Flavin Adenine Dinucleotide)[30].

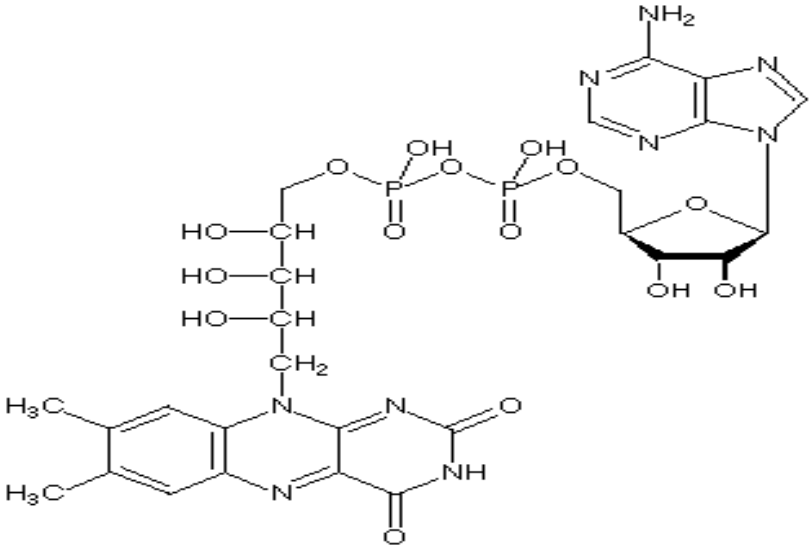

Schema 18 : structure of Flavin Adenine Dinucleotide

It has been suggested that MMOB may play a role in maintaining the integrity of the MMO enzyme, while being involved in facilitating the coordination of oxygen with the reduced form of MMOH, which is necessary to launch the catalytic cycle [38-42]. MMOH (methyl-coenzyme M reductase-hydroxylase) is a non-heme iron-containing metalloprotein that catalyzes the oxidation of methane to methanol.

3- Active site of MMOH hydroxylase

This dimer is composed of six polypeptide chains α2β2γ2 of 60/60/120A° in dimension. Each protomer is comprised of three αβγ subunits [38]. Interactions between the two protomers are primarily found between their two β subunits; the majority of these interactions occurring in the center of the dimer. There is no salt bridge between the two α subunits, though several interactions between the α and β subunits can be observed. The γ subunit does not participate in inter-protomer interactions, however, it is linked to both the α and β subunits by several Glu-Arg salt bridges [48]. The quaternary structure of MMOH is observed to take the form of a heart, with an axis of symmetry of order two [38]. Additionally, two iron-binding sites, located in each of the α subunits and separated by 45 Å, have been observed to contain two iron atoms each [33-39].

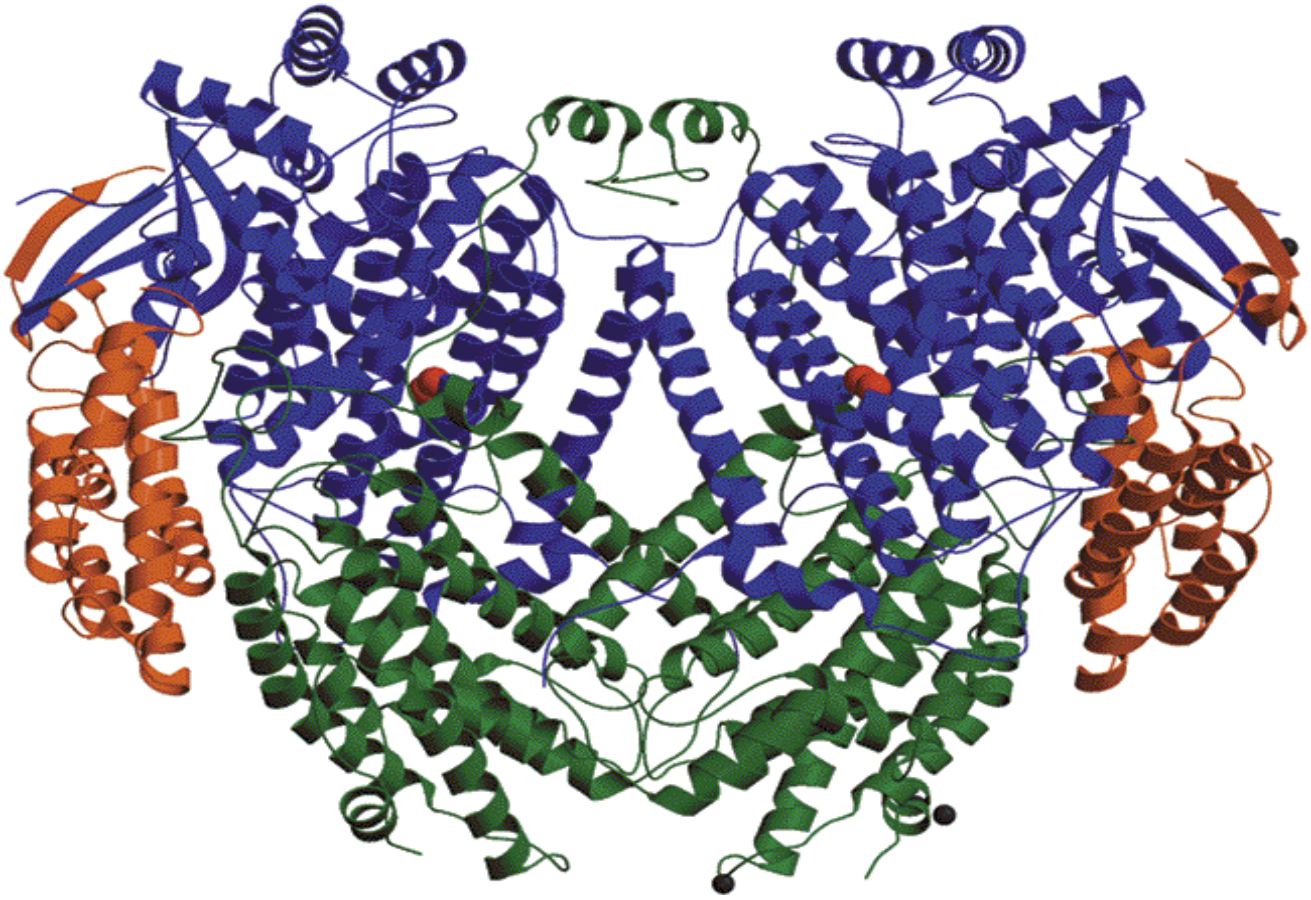

Figure 8: MMOH hydroxylase from Methylococcus Capsulatus sMMO, α subunits in blue, β subunits in green, and γ subunits in orange. Iron atoms and calcium atoms appear as red and dark blue spheres from the reference 39.

The two active sites have been characterized in multiple redox forms [44-49], and are located within a grouping of four alpha helices (αB, αC, αE, and αF). Certain amino acid residues of these helices are directly involved in the coordination of the iron dimer. Five different redox forms of MMOH have been characterized, with four diferric forms isolated from the enzymes Methylococcus Capsulatus and Methylosinus trichosporium OB3b, and one diferrous form isolated from the enzyme Methylococcus Capsulatus. The common feature of iron coordination among the hydroxylase isolated from Methylococcus Capsulatus is the presence of a histidine residue and several carboxylates from glutarate residues. Two distinct structures have been reported for the enzyme depending on the temperature at which the data were collected, i.e. 4°C (2.2 Å resolution) and –160 °C (1.7 Å resolution) [50-57]. The structure at 4°C showed two iron atoms linked by three bridges, namely a hydroxo, a μ-1,3-carboxylate of (Glu144), and an acetate, with the Fe-Fe distance being 3.4 Å. On the other hand, the structure at -160°C featured an aquo bridge in place of the acetate, resulting in a shorter Fe-Fe distance of 3.1 Å. The terminal ligands of both iron atoms were His147, Glu114 (monodentate), and OH2 for Fe1, and His246, Glu209 (monodentate), and Glu243 (monodentate) for Fe2. For the metallomulticopper oxidase of Methylosinus trichosporium OB3b, two distinct oxidized crystal forms were resolved at 2.0 and 2.7 Å [55-57]. One form contains two iron atoms connected by two hydroxo bridges or a hydroxo bridge and aqueous bridge (Figure 9B). The distance between the two iron atoms does not exceed 3 Å. The structure of MMOH from Methylococcus Capsulatus has been characterized, with the two hydroxo/aquo bridges decoordinated and Glu-243 shifted to bridge the two metals (Fe2 bidentate and Fe1 monodentate) [57-60]. This results in a major difference in the geometry around the iron, with the two metal centers now pentacoordinated.

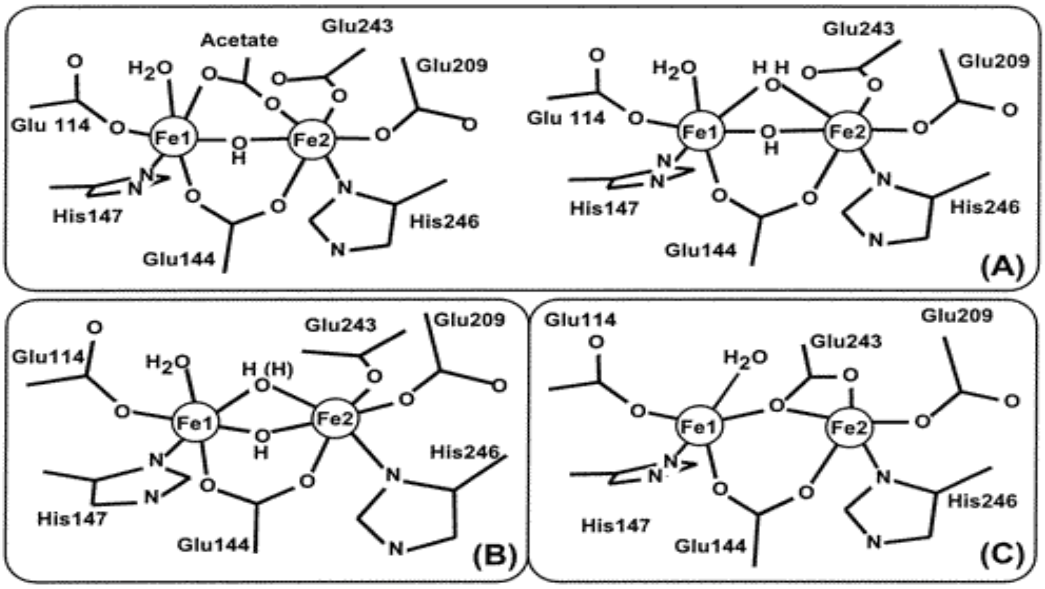

Figure 9: Active site view of hydroxylase structures of (A) Diferric MMOH (1MTY right and 1MMO) from *Methylococcus Capsulatus*, (B) Diferric MMOH (1MHY and 1MHZ) from *Methylosinus trichosporium*, (C) Diferrous MMOH from *Methylococcus Capsulatus*[59].

It has been proposed that the hydrophobic pockets present between the catalytic center and the second domain of the α subunit of the protein likely provide an access route from the substrate to the binuclear iron center, despite there being no direct path from the protein surface to the active site.

VII. REACTION MECHANISM

Based on kinetic and spectroscopic studies, it has been well-accepted that a multistep mechanism is involved in the oxidation of methane by non-heme iron-containing enzymes [60]. This process begins with the reduction of iron atoms from the resting di-ferric state to the di-ferrous state, catalyzed by the enzyme MMOHred. Following this, dioxygen is fixed, yielding the adduct species MMOHred*O2. Subsequently, oxidative addition of dioxygen to the metal occurs, generating the MMOHperoxo species. The denier derived from this is the precursor of the highly oxidizing compound MMOHQ, which is responsible for the hydroxylation of methane. Iron is present in this reaction in a high degree of oxidation. Contrary to some examples presented above, the oxygen reacts with the metal to form a highly oxidizing species, which then hydroxylates the substrate.

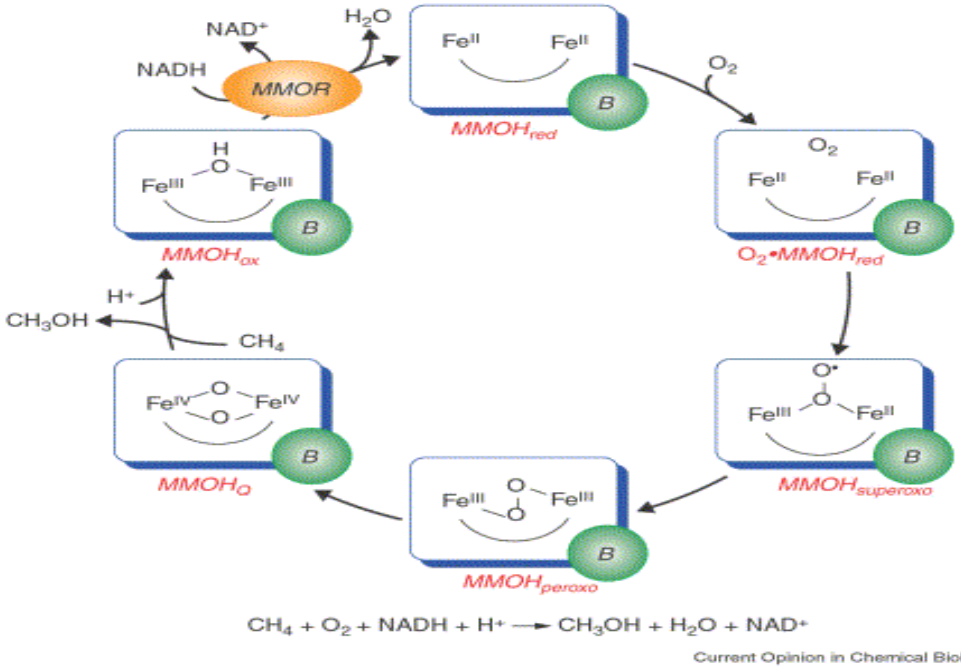

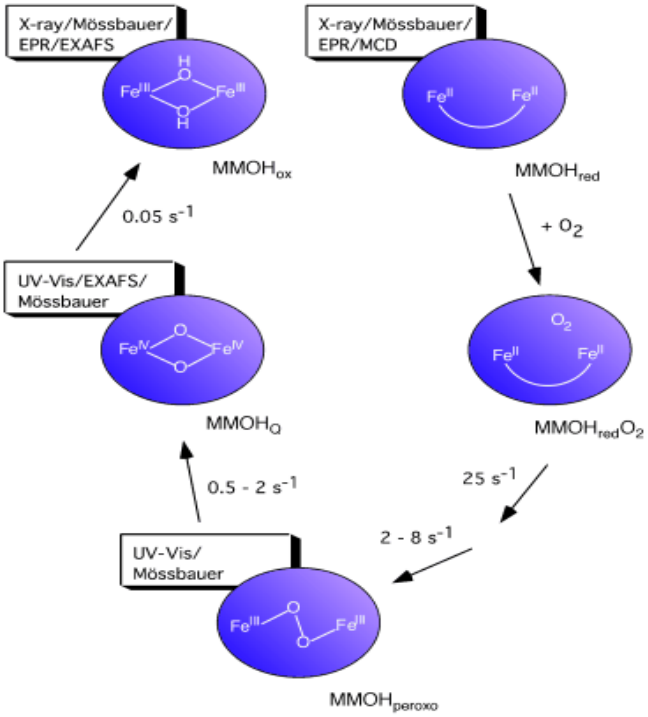

Schema 19: The reaction intermediates of the MMOH catalytic cycle, and some characterization methods.

VIII. CONCLUSION

Molecular oxygen and non-heme iron proteins are fundamental for human health and disease. They are necessary for proper cellular respiration and energy production, as well as protection from oxidative damage. Despite their critical role, knowledge of their structure and function is still limited, as is their association with various diseases. Continued research could potentially lead to improved comprehension and utilization of these proteins when treating and preventing diseases.

DECLARATION

Funding/ Grants/ Financial Support	No, I did not receive.
Conflicts of Interest/ Competing Interests	No conflicts of interest to the best of our knowledge.
Ethical Approval and Consent to Participate	No, the article does not require ethical approval and consent to participate with evidence.
Availability of Data and Material/ Data Access Statement	Not relevant.
Authors Contributions	I am only the sole author of the article.

REFERENCES

1. Machkour A, Thallaj NK, Benhamou L, Lachkar M, Mandon D.Chemistry. 2006 Aug 25;12(25):6660-8.P 6660-6661-6662-6663. [CrossRef]
2. Thallaj, N., Machkour, A., Mandon, D., Welter, R., New. J. Chem., 2005, 29, 1555 – 1558. [CrossRef]
3. Thallaj, N. K. Damascus University Journal for Basic Sciences. 34 (1) 2018.
4. Thallaj. N. K. Journal of AlBaath University (39) 2017.
5. Thallaj. N. K. Tishreen University Journal for Research and Scientific Studies 38 (6) 2016.
6. Thallaj NK, Rotthaus O, Benhamou L, Humbert N, Elhabiri M, Lachkar M, Welter R, Albrecht-Gary AM, Mandon D. Chemistry. 2008;14(22):6742-53.P6745-6746-6747.. [CrossRef]
7. Wane A, Thallaj NK, Mandon D. Chemistry. 2009 Oct 12;15(40):10593-602. P10594-10595-10595. [CrossRef]
8. Thallaj NK, Orain PY, Thibon A, Sandroni M, Welter R, Mandon D. Inorg Chem. 2014 Aug 4;53(15):7824-36. P7826-7827-7828. [CrossRef]
9. N. K. Thallaj, J. Przybilla, R. Welter and D. Mandon, J. Am. Chem. Soc. 2008, 130, 2414-2415. [CrossRef]
10. N. K. Thallaj, D. Mandon and K. A. White, Eur. J. of Inorg. Chem., 2007, 44–47. [CrossRef]
11. N. K. Thallaj, A. Machkour, D. Mandon and R. Welter, New J. Chem., 2005, 29, 1555–1558. [CrossRef]
12. Thallaj, N.; International journal of applied chemistry and biological sciences 2021, 2 (4), 65-77.
13. Thallaj, N.; Indian Journal of Advanced Chemistry (IJAC)2021, 1 (2), . [CrossRef]
14. Thallaj, N.; International Journal of Research Publication and Reviews (IJRPR)2021, 2, 10, 951-959
15. L. Labban, N. Thallaj, Z. Malek; International Journal of Medical Studies, 2020, 5, No 12, 23-36. [CrossRef]
16. L. Labban, M. Kudsi, Z. Malek, N. Thallaj; Advances in Medical, Dental and Health Sciences, 2020,3, 3,45-48. [CrossRef]
17. L. Labban, N. Thallaj, M. Al Masri; Journal of Advanced Research in Food Science and Nutrition, 2020,3,1,34-41. [CrossRef]
18. Thallaj, N; agha, M. I ,H;, nattouf; A.H; katib, CH; karaali, A; Moustapha, A; Labban L;open access library journal, 2020,7,5,1-21. [CrossRef]
19. L. labban; N. thallaj; A. labban; archives of medicine, 2020, 12, 2:8, 1-5. [CrossRef]
20. L. labban; N. thallaj; international journal of herbal medicine,2020, 8, 2, 33-37.
21. L. Labban, N. Thallaj, Z. Malek; Journal of Medical Research and Health Sciences, 2019, 2, 11, 784-787.
22. L. labban N. Thallaj; acta scientific nutritional health, 2019, 3,10, 7-12. [CrossRef]
23. Malek, Z.S.; Sage D.; Pevet, P.; Raison, S.; Endocrinology 2007, 148 (11), 5165-5173. [CrossRef]
24. Malek, Z.S.; Dardente, H.; Pevet, P.; Raison, S.; European Journal of Neuroscience 2005, 22 (4), 895-901. [CrossRef]
25. Malek, Z.S.; Pevet, P.; Raison, S.; Neuroscience 2004, 125 (3), 749-758. [CrossRef]
26. Malek, Z.S.; Labban, L.; The International Journal of Neuroscience, 2020, 1-7.
27. Malek, Z.S.; Labban, L.; European Journal of Pharmaceutical and Medical Research 2019, 6 (11), 527-532.
28. Malek, Z.S.; Journal of AlBaath University 2018, 40 (4), 39-62.
29. Malek, Z.S.; Tishreen University Journal for Research and Scientific Studies, 2018, 40.
30. ZS Malek, LM Labban; International Journal of Neuroscience, 2021,131 (12), 1155-1161. [CrossRef]
31. ZS Malek, LM Labban; Journal of current research in physiology and pharmacology, 2020, 4, (1),1-5.
32. L.M. Labban, M. M. Alshishkli, A. Alkhalaf, Z. Malek; J. Adv. Res. Dent. Oral Health, 2017, 2(3&4), 1-4.
33. L Labban, ZS Malek, Open Access Library Journal, 2018, 5 (07), 1-11. [CrossRef]
34. L Labban, ZS Malek, Ann Food Nutr Res J, 2019,1 ,1
35. Labban, L. and N. Thallaj, 2019. Acta Scient. Nutr. Health, 3: 7-12. [CrossRef]
36. A Abbood, C Smadja, C Herrenknecht, Y Alahmad, A Tchapla, M Taverna Journal of Chromatography A 1216 (15), 3244-3251 [CrossRef]
37. A Abbood, C Smadja, M Taverna, C Herrenknecht Journal of Chromatography A 1217 (4), 450-458 [CrossRef]
38. A Abbood, C Herrenknecht, G Proczek, S Descroix, J Rodrigo, M Taverna,Analytical and bioanalytical chemistry 400 (2), 459-468 [CrossRef]
39. A Abbood, C Smadja, M Taverna, C Herrenknecht Journal of Chromatography A 1498, 155-162. [CrossRef]
40. Y. alhomush, Z. malek, A. Abboud, N.Thallaj, Research Journal of Pharmacy and Technology, 2022, 15, 10.

41. N.Thallaj, Tishreen university journal,2022,44, 1, 59-77.
42. N.Thallaj, Tishreen university journal,2022,44,2, 87-105.
43. Z. Malek, H. Dardente, S. Raison, P. Pevet, Mesocricetus auratus neuronal tryptophan hydroxylase mRNA, partial cds, 2003, GenBank, AY345967.1.
44. N.Thallaj. Indian journal of advanced chemistry, 1, 3, 2022. 10-14. [CrossRef]
45. N.Thallaj.Xi'an ShiyouDaxueXuebao (ZiranKexue Ban)/ Journal of Xi'an Shiyou University, Natural Sciences Edition.2022.65, 06. 289-301.
46. A. Abbood, N Thallaj, (2023). 7,(1), Arab Journal of Pharmaceutical Sciences.
47. N Thallaj, (2023). 44,(6),21-29. Tishreen University Journal-Medical Sciences Series.
48. A.Abbood, Z.Malek, N.Thallaj. 2022 15, 11, 4935-4939. Research Journal of Pharmacy and Technology. [CrossRef]
49. A.Abbood, Z.Malek, Y.Al-Homsh, N.Thallaj. 2022 15, 10, 4727-4732. Research Journal of Pharmacy and Technology. [CrossRef]
50. N Thallaj, (2023). 45,(1). Tishreen University Journal-Medical Sciences Series.
51. A.Abbood, N Thallaj, (2023). 45,(2). Tishreen University Journal-Medical Sciences Series.
52. L. Alallan, M. Khazem, N Thallaj, (2023). 45,(1). Tishreen University Journal-Medical Sciences Series.
53. L. Alallan, Z.malek, (2023). 45,(1). Tishreen University Journal-Medical Sciences Series.
54. Kappock, T. J; Caradonna, J. P.; Chem.Rev. 1996, 96, 2659-2756. [CrossRef]
55. Heidi, E.; Bjorgo. E.; Flatmark T.; and Stevens R. C.; Biochimistry 2000, 39,2208-2217. [CrossRef]
56. Solomon, E. I.; Brunold, T. C.; Mindy I. D.; Kemsley, J. N.; Sang-Kyu Lee.; Lehnert, N.; Neese, F.; Skulan, A. J.; Yi-Shan Y.; and Jing Z.; Chem.Rev. 2000, 100, 235-349. [CrossRef]
57. Goodwill, K. E.; Sabatier, C.; and Stevens, R. C.; Biochemistry 1998, 37, 13437-13445. [CrossRef]
58. Wang Lin.; Erlandsen, H.; Haavik, J.; Knappskog, P. M.; and Stevens R. C , Biochemistry 2002, 41, 12569-12574. [CrossRef]
59. Nordlund P.; in Handbook of Metalloproteins (Eds.: I. Bertini,A. Sigel, H. Sigel), Marcel Dekker, *New York*, **2001**, *pp*. 461 -570. [CrossRef]
60. Xia, T.; Gray, D. W. ; Shiman, R. J.; Biol. Chem. 1994, 269, 24657-24665. [CrossRef]

AUTHOR PROFILE

Dr. Nasser Thallaj
PhD in Chemical Sciences, Assistant Professor
Member of American Chemical Society (ACS)
E-mails: nasserthallaj@gmail.com

2020- presente time: professor in the biomedical Science program.
2020- Present time: Assistant professor position. Faculty of pharma *alrashed university*, Damascus, Syria
From 15 june 2019 – 31 July 2020: President of *AlJazeera University*, Damascus, Syria.
From Abril 1st 2019 – 15jun: vice president for scientific affairs and Dean of Faculty of pharmacy AlJazeera University, Damascus, Syria.
From October 1st 2018-15 march 2020: Dean of Faculty of pharmacy *AlJazeera University*, Damascus, Syria.
2017-31 July2020: *Assistant professor* position. Faculty of pharmacy, *AlJazeera University*, Damascus, Syria
- 2015-2017: *Assistant professor* position. Faculty of pharmacy, *Syrian Private University*, Damascus, Syria
- 2015- 2016: Consultant in Ugarit Education Group: foundation of *AlManara University*.
- 2014-2015: vice president for scientific affairs (in charge), *University of Kalamoon*, Dier Attieh, Syria.
- 2014-2015: In charge of higher education affairs, *University of Kalamoon*, Dier Attieh, Syria.
- 2012-2014: Dean of Faculty of applied Sciences, *University of Kalamoon*. Dier Attieh, Syria.
- 2010-2013: Head of Department of Chemistry. Faculty of applied Sciences, *University of Kalamoon*. Dier Attieh, Syria
-2008: *Assistant professor* position. Faculty of applied Sciences, *University of Kalamoon*. Dier Attieh, Syria
2007-2008 : Post-Doctoral position. *Laboratory of NanoOrganic Chemistry, and Supramolecular Materials*, thesis title : *drug delivery system Department* of Chemistry. *University Notre Dame de la Paix*. Namur, Belgium.